Journal of Bioscience and Bioengineering
VOL. 128 No. 2, 209–217, 2019

ELSEVIER

www.elsevier.com/locate/jbiosc

Time-course colony tracking analysis for evaluating induced pluripotent stem cell culture processes

Kei Yoshida,[1] Mika Okada,[1] Risako Nagasaka,[1] Hiroto Sasaki,[2] Mai Okada,[1] Kei Kanie,[1] and Ryuji Kato[1,3,4,*]

Department of Basic Medicinal Sciences, Graduate School of Pharmaceutical Sciences, Nagoya University, Furocho, Chikusa-ku, Nagoya 464-8602, Japan,[1] Department of Biotechnology, Graduate School of Engineering, Nagoya University, Furocho, Chikusa-ku, Nagoya 464-8602, Japan,[2] Stem Cell Evaluation Technology Research Association (SCA), Hacho-bori, Chuou-ku, Tokyo 104-0032, Japan,[3] and Institute of Nano-Life-Systems, Institute of Innovation for Future Society, Nagoya University, Division of Micro-Nano Mechatronics, Furocho, Chikusa-ku, Nagoya 464-8602, Japan[4]

Received 17 October 2018; accepted 16 January 2019
Available online 7 February 2019

Increasing the yield and maintaining a high quality of induced pluripotent stem cells (iPSCs) is necessary for manufacturing iPSCs at the industrial scale. However, because iPSCs are delicate, it is important to evaluate their quality during processing. To examine the status of cultured iPSCs non-invasively, morphology-based iPSC colony evaluation may be an efficient technology for cellular status monitoring and analysis. In this study, we examined the effectiveness of time-course colony tracking analysis for evaluating the iPSC culture process. Particularly, we obtained detailed time-course data to evaluate the effect of the pipetting technique on cell dissociation before seeding. Although the pipetting process causes severe shear stress to cells, which affects their quality, these effects have not been quantitatively analyzed because of their complex and uncontrollable parameters. By analyzing the heterogeneity and time-course responses of individual colonies, our colony tracking analysis revealed a critically damaged population caused by pipetting stress which could not be detected in conventional bulk analysis. Moreover, by comprehensively analyzing colony tracking data, which links the time-course morphology and marker staining results with each colony, we found that colony morphology is only highly correlated with the undifferentiated marker in the final stage, with a lower correlation in the early stages. Thus, colony tracking analysis provides a way to quantify cellular morphological information when evaluating complex iPSC manufacturing processes.

[**Key words:** Quality monitoring; Induced pluripotent stem cell; Morphology analysis; Colony tracking analysis; Cell quality evaluation; Pipetting technique; Cell yield]

Because of their multi-lineage differentiation and self-renewal abilities, induced pluripotent stem cells (iPSCs) are considered ideal cell sources for research in regenerative medicine (1,2) and drug development (3–5). To expand the applications and global availability of iPSCs, it is critical to manufacture high-quality iPSCs at an industrial scale (6). Deviation in the quality of iPSCs can cause unexpected manufacturing risks, such as low efficiency in the differentiation process for obtaining the objective lineage or insufficient cellular yield, which alters production costs (7). Highly controlled iPSC cultures contribute not only to their industrial production, but also to safer and more reproducible cellular applications.

Although there have been advances in stabilizing their culture conditions, stable and reproducible quality control of iPSCs is not technically easy to perform. One reasons for this is the lack of technologies enabling detailed in-process measurements. To manufacture cellular products within the controlled range of objective quality, it is critical to monitor the cell culture status using more data to quantitatively understand controllable parameters. In addition to conventional expert-guided cell culture, which greatly relies on the experience and unwritten technical knowledge of experts, cell manufacturing facilities are now investigating their culture processes by using detailed monitoring technologies (8,9). Imaging technology is among the most practical and promising methods for quality evaluation.

Compared to conventional end-point assay techniques, imaging is non-invasive and can be used to evaluate the real-time cellular status from the start to the end of the cell culture process (10–12). Continuous evaluation is particularly advantageous in the large-scale manufacturing of cell products, as detecting irregular events can prevent the failure of costly culture processes and formation of undesirable products. Additionally, studies have suggested that the morphological signature is an important factor in the success of stem cell culture (13).

Previous studies showed that colony morphology is highly correlated with the pluripotent cellular status of iPSCs and can be used as a non-invasive indicator for quality evaluation (14–16). Compared to bulk evaluation techniques such as quantitative polymerase chain reactions or microarrays, immunostaining for cell surface markers, and teratoma assays (17–19), image-based evaluations be used to examine individual colonies or cells, which is highly advantageous for evaluating a heterogenic group of cells.

* Corresponding author at: Department of Basic Medicinal Sciences, Graduate School of Pharmaceutical Sciences, Nagoya University, Furocho, Chikusa-ku, Nagoya 464-8602, Japan. Tel.: +81 52 747 6811; fax: +81 52 747 6813.
E-mail address: kato-r@ps.nagoya-u.ac.jp (R. Kato).

1389-1723/$ – see front matter
https://doi.org/10.1016/j.jbiosc.2019.01.011

Our group previously reported the concept of evaluating iPSC quality by examining morphology (20–22). In these previous studies, we found that multiple morphological parameters extracted from phase-contrast colony images can be used to define morphologically irregular colonies, which also show irregular gene expression and marker expression profiles, among a heterogeneous group of colonies.

Although the performance of iPSC colony evaluation techniques were demonstrated to be efficient, various factors have not been thoroughly evaluated to determine the effectiveness of image-based iPSC culture technology in cell manufacturing processes.

First, the techniques/skills used in culture processes should be evaluated. Compared to established biological assays, techniques and skills used in cell culture are typically difficult to evaluate. One reason for this is the large number of influential parameters, making combinatorial evaluation difficult. The other reason is that some of these factors are difficult to quantitatively evaluate. Additionally, the effects of techniques and skills in cell culture may appear over time; thus, these factors cannot be measured using only end-point assays. For this complex task, image analysis is a powerful tool that enables morphological quantitation during the course of the culture process. In our previous study, we showed that such technical differences can be compared by visualizing morphological clustering of iPSC colonies (21). However, other more practical techniques/skills in cell manufacturing have not been analyzed by image analysis.

Second, for image-based iPSC culture analysis, the most effective evaluation period should be established. Although the cost of imaging is lower than that of conventional assays, unplanned image acquisition can increase computational costs. Moreover, knowing which time-point during the manufacturing process is the most reliable for determining the quality of iPSC colonies is important.

Third, previous studies, including those by our group, have shown that morphological parameters can be used to non-invasively evaluate iPSC colony quality (including marker expression) (20–22). However, in these studies, the morphological parameters were measured over time using bulk colonies rather than from colony tracking data. Therefore, prediction models trained by such morphological data reveal the relationship between morphology and marker expression, but the data are from different colonies. In contrast, in our colony tracking data, all time-course morphological information and staining results were linked to the same colony. This dataset makes it possible to precisely evaluate which morphology is the most important at which time. A detailed examination of morphological parameters by constructing a machine-learning model for predicting iPSC colony quality has not been reported to date.

In this study, we examined these issues for the further application of image-based iPSC colony evaluation technology for evaluating cell manufacturing processes.

First, to assess the technical differences in iPSC culture processes, we focused the effect of pipetting on cell dissociation. Pipetting is one of the most basic cell-handling techniques and is essential for dissociating aggregated cells after centrifugation before seeding. Although the cells are subjected to severe shear stress during this process (23), how to optimize this process to yield the best conditions for iPSCs remains unclear. It is also very difficult to quantify the stress exerted on the cells because of various minor variations and different equipment used, which can alter the fluid mechanics. More complex parameters alter the shear stress towards cells during this process, such as the stiffness of the cell pellet, size and shape of the centrifugation tube, distance between the end of the tip and bottom of the tube, speed of aspiration and dispensing. Therefore, the protocol for pipetting is commonly described non-quantitatively, resulting in large differences between the performances of various personnel. By mimicking the differences between rough and delicate pipetting manipulations, we investigated how much information image-based evaluation can provide when examining the efficiency and stability of the manufacturing process.

Second, we conducted colony tracking analysis of iPSCs (Fig. 1). Recent image analysis technology not only enables the measurement of morphological parameters for individual colonies, but also allows for the same cell/colony to be tracked throughout culture. Because iPSC colonies do not largely migrate two-dimensionally after reaching a certain size, tracking their time-course is more feasible than tracking individual migrating cells. Therefore, colony tracking can provide additional information during image-based evaluation. Some reports have indicated the importance of colony tracking information in effective manufacturing of iPSCs. Therefore, we examined the advantages of colony tracking and discussed its effective usage for monitoring of iPSC manufacturing processes.

MATERIALS AND METHODS

Cell and cell culture The human iPSC line 201B7 and sub-clones 201B7-1A and TIG108-4f3 (iPS-TIG108-4f3 (RRID:CVCL_DP61)) were provided by the Center for iPS cell Research and Application, Kyoto University. Both 201B7-1A and TIG108-4f3 were used as potentially irregular cell lines because 201B7-1A is a subclone that gained an additional copy of chromosome 12 after prolonged culture and its parent, healthy 201B7, and TIG108-4f3 are subclones analyzed to detect differentiation-defective profile. iPSCs were maintained in knockout DMEM/F-12 (Life Technologies, Carlsbad, CA, USA) supplemented with 0.1 mM non-essential amino acids (Life Technologies), 0.1 mM 2-mercaptoethanol (Life Technologies), 2 mM L-glutamine (Life Technologies), and 20% knockout serum replacement (Life Technologies) on murine embryonic fibroblasts feeder cells (Merck Millipore, Billerica, MA, USA) at 37°C and 5% CO_2. The feeder cells (Passage 3) were thawed and seeded at a concentration of 6.8×10^4 cells/well into 6-well plates (Corning Life Sciences, Corning, NY, USA). Two days after seeding the feeder cells, iPSCs were seeded on the feeder cells at a split ratio of 1:4. The medium was replaced every two days with medium containing 10 ng/mL basic fibroblast growth factor (Life Technologies). When iPSCs were cultured for 7 days, the cells were treated with 1 mg/mL Dispase II (Roche Applied Science, Basel, Switzerland) for 2 min and collected using a cell scraper. All conditions were treated with same scraper procedure to minimize the effect of cell scraping among samples. The collected cells were suspended under different conditions of pipetting using a motor-assisted auto pipetter (Drummond Company, Inc., Birmingham, AL, USA) to minimize manual handling bias.

Marker staining of colonies Seven days after seeding the iPSCs, the undifferentiation staining lectin marker rBC2LCN-635 (100-fold diluted; Wako Pure Chemical Industries, Ltd., Osaka, Japan) was mixed with new medium and the cells incubated in this medium for 2 h at 37°C, 5% CO_2 for labeling. For immunestaining of undifferentiation/differentiation markers, the cells were washed with phosphate-buffered saline (PBS) (Nissui Pharmaceutical Co., Ltd., Tokyo, Japan) and fixed for 15 min in 2% paraformaldehyde (Wako Pure Chemical Industries, Ltd.). The cells were washed with PBS and permeabilized in PBS containing 1% bovine serum albumin (Wako Pure Chemical Industries, Ltd.) and 0.5% Triton-X-100 (Wako Pure Chemical Industries, Ltd.) for 30 min. Next, the cells were hybridized with two primary antibodies, OCT3/4 mouse IgG (50-fold diluted; Santa Cruz Biotechnology, Dallas, TX, USA) and vimentin rabbit IgG (500-fold diluted; Abcam plc., Cambridge, UK), overnight at 4°C. The cells were hybridized to two secondary antibodies, Alexa Fluor 488 Goat Anti-Mouse IgG (H + L) (1000-fold diluted; Cell Signaling Technology, Danvers, MA, USA) and Alexa Fluor 488 Goat Anti-Mouse IgG (H + L) (1000-fold diluted; Cell Signaling Technology), for 2 h at 25°C. Only vimentin staining was used to confirm the state of colonies that had lost staining of either OCT3/4 or rBC2LCN.

Image acquisition Phase-contrast and fluorescence images of iPSCs were acquired with a BioStation CT (Nikon Corp., Tokyo, Japan) at 4× magnification. The image acquisition field was set to an area of 1.6 cm^2 in the center position, consisting of 8 × 8 tiling images; the images were acquired by automatic focusing. All phase-contrast images were acquired once every 6 h, from 2 to 7 days after seeding the cells.

Image processing All microscopic images were processed and quantified using CL-Quant software version 3.10 (Nikon Corp.). The iPSC colonies in the images were recognized in 6 steps: background adjustment (step 1), segmentation of iPSC colonies (step 2), filling in blank holes (step 3), removal of noise (diameter <225 μm, step 4), applying constructed filter-sets (1–4 processing) to the raw image (step 5), and measurement of colony morphology (step 6) (Fig. S1). Morphological profiles using 16 parameters (area, compactness, perimeter, shape factor, inner radius, equivalent radius, rod-like width, mean intensity, median

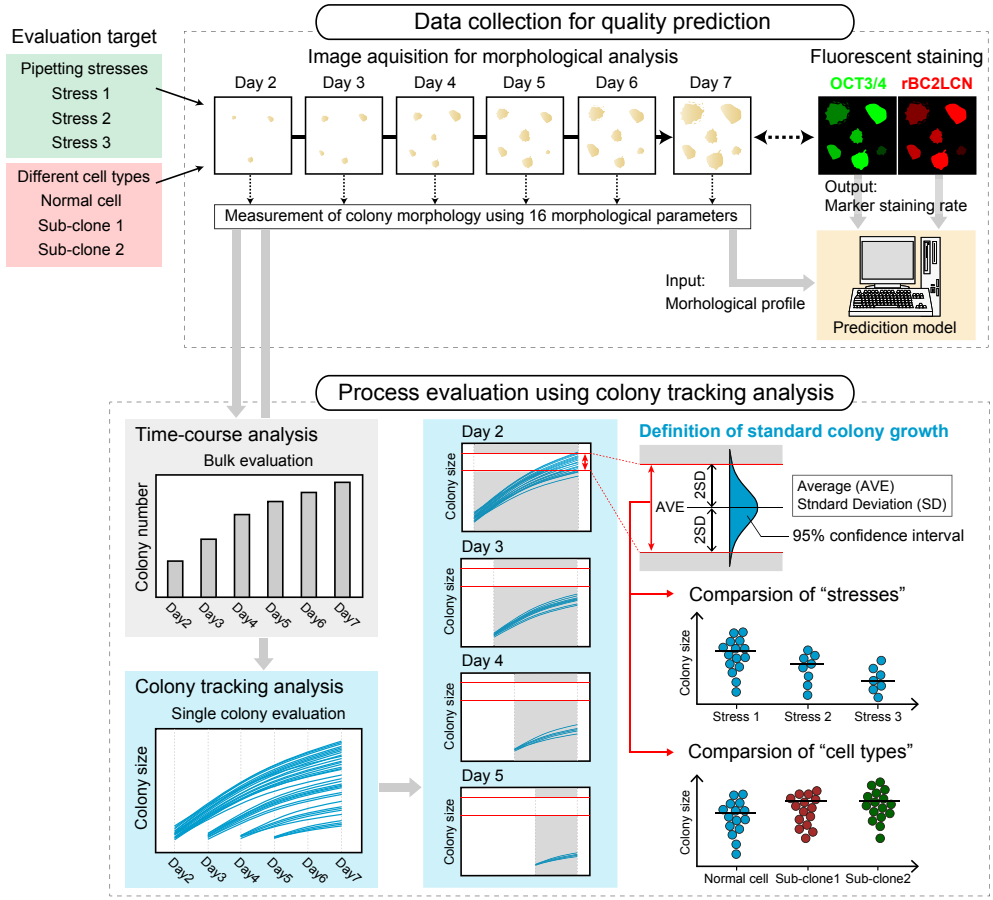

FIG. 1. Analytic scheme of time-course colony tracking analysis in this study. The effect of pipetting stress was evaluated as the target application. During the collection of quality prediction data, phase-contrast microscopic images were acquired during cell culture (days 2–7). Images were processed to measure colony morphologies using 16 morphological parameters. Marker staining results (OCT3/4 and rBC2LCN) were evaluated as the quality criteria on the final day. Using the morphology profile (input) and marker staining rate (output), a machine-learning model was constructed to predict the colony quality only from morphology. In parallel to model construction, colony image data was analyzed by colony tracking analysis. For comparison, conventional colony counts in bulk evaluation were evaluated. Recognized colonies in the images were tracked throughout the time-course to link the time-course morphological profiles and final biological evaluation result. Compared to the conventional colony counts, the colony tracking data visualizes three important aspects: (i) sub-populations that start growing at different times, (ii) individual growth curves, and (iii) colony size distribution at the end. When the 95% confidence interval is defined as a range criterion of standard colonies, differences between the stresses and cell lines can be quantified.

intensity, standard deviation of intensity, CV intensity, correlation, energy, entropy, homogony, inertia) were measured from recognized cellular objects. The growth of single colonies was measured by a tracking algorithm following the manufacturer's protocol. To stabilize our analysis, we defined a diameter of 225 μm as the minimum recognition size. The time-point when the colonies reached this size was recognized the start of the tracking process.

Prediction model construction The morphological profiles obtained from phase-contrast images were used to construct two regression models to predict the areas positive for undifferentiation markers (OCT3/4 and rBC2LCN-635). The least absolute shrinkage and selection operator (LASSO) regression models trained with input data (morphological profiles) were used in combination with output data (differentiation rates of each colonies, which was determined by quantifying the marker staining area normalized to their colony size by image analysis). The two regression models were constructed using different training datasets (OCT-3/4: 59 colony tracks; rBC2LCN: 99 colony tracks which single colony can be tracked clearly during 2–7 days). The average of colony size with the staining result was 910 μm diameters. Each dataset was produced by end-point undifferentiation marker staining; therefore, two prediction models were constructed: (i) prediction model for OCT3/4 (predicts the OCT3/4 staining rate at day 7 using morphological profiles from 2 to 7 days) and (ii) prediction model for rBC2LCN (predicts the rBC2LCN staining rate at day 7 using morphological profiles from 2 to 7 days). For comparative analysis, optional prediction models that could predict either OCT3/4 or rBC2LCN at day 7 from the single morphological parameter (area of day 7) were constructed by linear regression.

Additionally, to investigate the best predictive performance of the period for acquiring morphological information, the total time-course usage of morphological data was examined within various window sizes, and model performance was examined. The prediction accuracies were compared using the rooted mean square error (RMSE) value, which is the difference between the predicted value and experimentally determined value. A lower RMSE value indicates a higher prediction performance. When RMSE values were within the range of the mean ± standard deviation (SD) of the experimental data, the prediction was considered as correct in accuracy calculation. The performance of each prediction model was evaluated by leave-one-out cross-validation. R (version 3.1.0) (R Development Core Team, https://www.r-project.org/) was used for this analysis.

RESULTS

Colony tracking analysis for evaluating the cell yield under different pipetting conditions To investigate the effectiveness of image-based iPSC colony evaluation for the practical application in the manufacturing process, we focused on the effects of pipetting on iPSCs as a model for assessing culture techniques (Fig. 1). During iPSC culturing using both culture methods, including clump-type seeding or single cell-type seeding, pipetting to dissociate the cell pellet is a basic but technically critical process. We evaluated the complex effects of this technique on the cells by using detailed colony tracking analysis to quantify the cellular morphological changes.

To mimic the differences between different pipetting techniques, we used three levels of pipetting conditions: 5-times pipetting (shear stress level; low), 10-times pipetting (shear

stress level; medium), and 15-times pipetting (shear stress level; high) using a motor-assisted auto pipetter. After pipetting, the cells were seeded and cultured for 7 days, followed by time-course image acquisition for image analysis.

First, we evaluated the yield of cells as the first simple criterion for iPSC quality. Cell yield is a critical quality criterion that can alter the culture costs associated with cell manufacturing. To evaluate the differences in cell yield among pipetting conditions, colonies were recognized in each image obtained during the total time-course (Fig. 2A), and the total colony areas were plotted against the time course as an example of conventional bulk colony counts (Fig. 2B). The total area decreased depending on the level of shear stress, resulting in an unexpected loss of cell yield on the final day. However, the size distribution of colonies was not interpretable from these colony number data. Thus, conventional bulk colony count data do not reveal population changes in the yielded cells.

To further evaluate this image-based information, we next analyzed the same time-course image data using the single-colony tracking technique (Fig. 3, analysis concept illustrated in Fig. 1). By comparing these data to the former data, we examined the effectiveness of tracking-based analysis for understanding the detailed culture status. Through tracking analysis, several novel aspects that are not observed in bulk analysis were found.

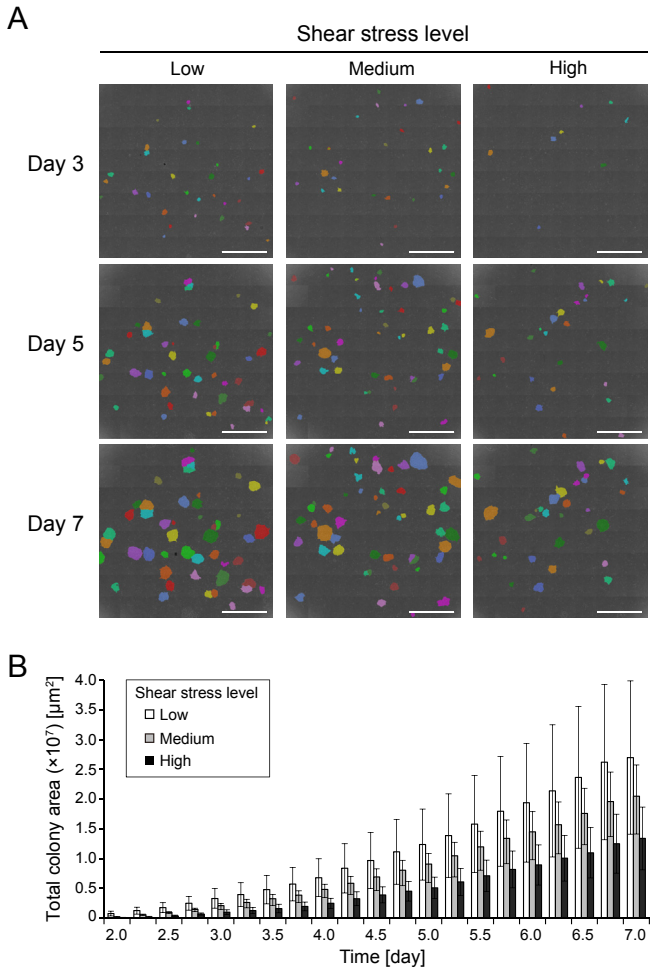

FIG. 2. Bulk colony counts showing the pipetting effect on iPSC dissociation before seeding. (A) Time-course microscopic images under three shear-stress conditions. Individual colonies in the images were recognized by image processing and indicated with colored masks. The colored masks in the image indicate that colonies were independently recognized and labeled by the image processing. Within the same image, the mask color was defined randomly using the color panel in the software. When colony numbers exceeded the number of color panels, the same color panel was repeated. By tracking, the same color was given to the same colony across the culture period. Scale bar: 4 mm. (B) Conventional visualization of time-course total colony area with different pipetting stresses. The color of the bar indicates the shear stress level: open bars; low; shaded bars, medium; and closed bars, high. Error bars indicate means ± SD for 4 independent images.

When tracks for each colony (colony growth curves) were extracted from the image data, heterogenic varieties of colonies under the same conditions were clearly visualized. In addition to the size distribution of colonies on the final day, the colony tracking data revealed individual time-course growth profiles.

From starting point information, the track data revealed wave-like growth patterns, which are sub-populations of colonies recognized as tracks with time-differences (Fig. 3A). We detected early-recognized colonies (which suggest fast-growing cells) and late-recognized colonies (which suggest late-growing cells) in the same seeded cells. From this information, fast-recognized colonies were found to be the major sub-population that was decreased by higher-strength pipetting. Although there was a correlation between the increased sub-population of the later-recognized colonies and level of pipetting stress, the number of colonies in this sub-population was minor and thus not detected among the cells.

From the individual gradients of tracks, individual colony growth profiles were evaluated in detail. When the gradients were compared throughout the culture process, we found that the growth rates of each colony did not show large differences for the different pipetting stresses. When all colony tracks were summarized, including colonies from fast-recognized and late-recognized cells, their basal growth rates were not found to be greatly affected. Additionally, there were no exceptional colonies that were recognized in the later period that subsequently showed extremely high growth to overwhelm the other colonies.

These results demonstrate that the most critical effect of the dissociation of iPSCs by pipetting is the reduction of fast-recognized cells which reached the minimum recognition size (see the definition in Materials and methods) early in cell culture rather than lowering individual cell growth rates. This result means that fast-recognized cells could form colonies early, in other words, the stress of pipetting decreased cells' colony-formation ability. When we analyzed large colonies (>1000 μm diameter) at the end of the culture (day 7), more than 90% of colonies were found to have originated from the early period (days 2–3) (Table S1). The number of matured-size colonies on day 7 reflects the number of intact fast-recognized cells after seeding; the late-recognized cells only disturb the size homogeneity in the final yielded colonies.

Colony tracking analysis to compare the stability of productivity In cell manufacturing, it is important to evaluate not only the yield, but also the stability of productivity. Because colony size homogeneity was found to be important for stable cell yield, we next investigated the usage of colony tracking data to standardize the range of sizes of the obtained colonies (Fig. 3B).

iPSCs' marker staining results differs because of both their quality loss and their maturation rate; thus, we analyzed the marker expression rate in approximately 380 colonies of different sizes (225–1760 μm diameter) under undifferentiation culture conditions (Fig. S2). The results confirmed that the single colony marker expression rate greatly varied according to colony sizes. Even after the same culture period (day 7) under undifferentiated culture conditions, smaller-sized colonies (<800 μm diameter) expressed a high level of the differentiation marker vimentin, while larger colonies (>1400 μm diameter) showed lower expression. When larger colonies were compared, morphologically irregular colonies showing a fibroblastic cellular morphology in their periphery and no undifferentiation marker expression showed clear vimentin expression. Thus, when vimentin is used to label irregularly differentiating colonies even in an undifferentiated state, only large colonies show reliable staining results. Similarly, the marker

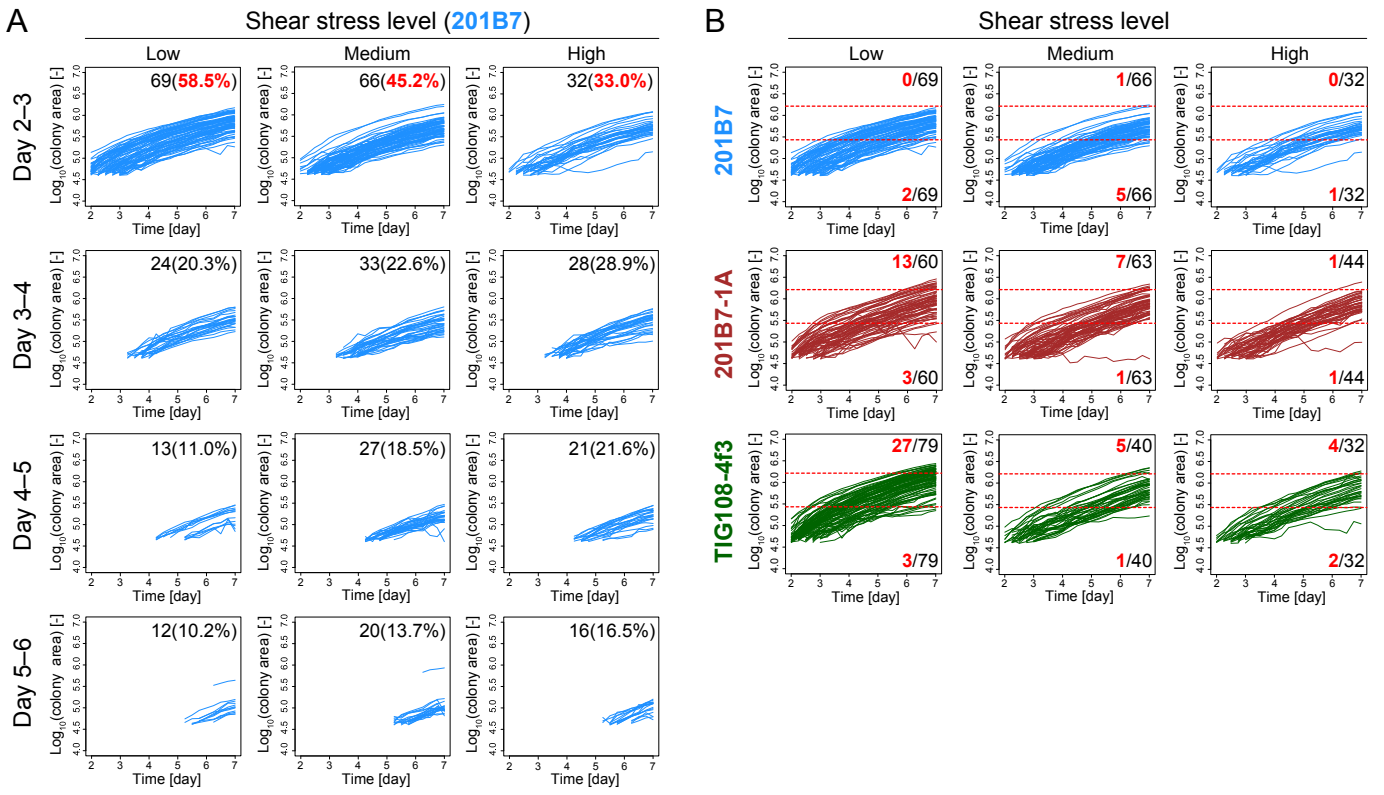

FIG. 3. Colony tracking analysis for evaluating iPSC colony yield. (A) The heterogenic colony size distribution was obtained from the end of colony tracks. (B) Comparison of pipetting effects by colony track data. Colony tracks were separated based on their starting time-differences. The number in the upper right on the plot indicates the number of colonies recognized as tracks in each period and its rate in the total colonies over the total time. X-axis: time; Y-axis: size of single colony area. The red horizontal lines indicate the range of standard colony sizes defined by the statistical confidence interval of 201B7 with low pipetting stress (defined as average ± 2SD of colony size at day 7). When the colony track was higher/lower than the defined range of colony sizes, it was regarded as an irregular colony. The numbers in the upper right and lower right of the plot indicate the number of irregular colony tracks (red) within the total tracks (black).

staining results of the conventional undifferentiation marker OCT3/4 were not consistent when the colony sizes differed. Even under the same culture conditions, OCT3/4 expression was low in small colonies and high in larger colonies. Moreover, homogeneous expression was disrupted when the colony size became too large. This result also demonstrates the complexity of interpreting marker staining results. With OCT3/4, the staining result can be trusted for detecting irregularly deviated colonies from their status only when colonies are in a certain size range.

Because colony tracking data can be used to analyze selected colonies that clearly examined from the start until the end of culture, these data were considered to show less noise or bias in image analysis. Therefore, we applied this data to define the range of standard colony growth. As a model, we selected the 201B7 clone under low shear stress and defined the standard range of colony sizes from the 95% confidence range (average $\pm 2\times$ SD) of 69 colony tracks (Fig. 3B). Statistically, larger/smaller colonies not in this range were considered to have a rare size. Such rare-size colonies are not necessarily bad colonies that do not adhere to any of the quality criteria; however, these colonies may disturb the homogeneity of quality criteria.

By defining a standard range of yielded colony sizes, comparison between two sub-clones (201B7-1A and TIG108-4f3) with irregular biological characters indicated that a certain rate of overgrown colonies occurred even under the same culture protocol (Fig. S3). Approximately 2–34% of colonies of these sub-clones may show deviated sizes in the final product, which can disturb the objective quality homogeneity.

Defining a standard size range is also important for understanding the sensitivity of each strain to pipetting stress. There were more immature/overgrown colonies in case of the two sub-clones, resulting in the formation of deviated colonies with sizes outside the standard range.

Informational content of morphological parameters of iPSC colonies for efficient image-based undifferentiated marker prediction When the yield and the size of the colonies can be controlled with support from image analysis, the marker expression potential of each colony is the next important criterion to consider in cell manufacturing.

To construct a morphology-based iPSC colony quality prediction model, we collected tracking data and end-point marker staining data (OCT3/4 and rBC2LCN at day 7) (Fig. 4). We only collected the marker staining results of colonies >910 μm in average diameter. To quantitatively predict such quality marker expression rates, we measured the marker staining rate of each colony (day 7), and combined these data with the time-course data of 16 morphological parameters (refer to Materials and methods for details) (2–7 days) for machine learning (concept illustrated in Fig. 1).

To understand the most effective usage of the time-course data, we examined different window-sizes for morphological data usage in the prediction. First, use of the morphological profile at each time-point was compared to the prediction error rate (Fig. 5A). As a result, to predict the expression rate of both markers, the morphology during the most recent time-point, which was close to the marker staining time-point, showed the best prediction accuracy. Second, time-point data were combined from the earlier period for prediction (Fig. 5B). Combining the morphological time-course data did not increase prediction accuracy compared to the most recent single time-point usage shown in Fig. 5A. Third, time-

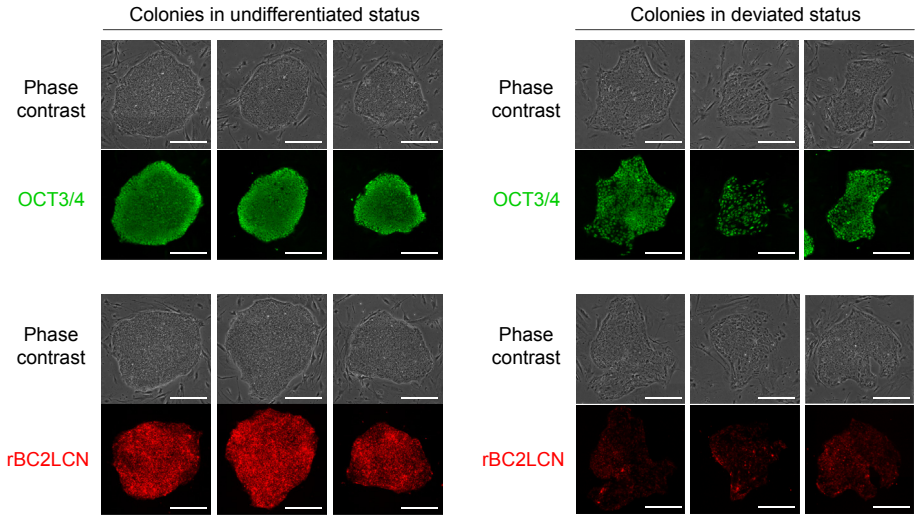

FIG. 4. Representative images of iPSC colony morphologies and their marker expression. The colonies were stained with OCT3/4 (green) and rBC2LCN (red) using the technique of immunofluorescence. Scale bar: 400 μm.

course data were eliminated from the earlier period to examine whether there was noise in the earlier morphologies that resulted in a lower prediction accuracy after combining the data in Fig. 5B, C. However, the prediction accuracy did not recover when considering such early noises, and the most recent time-point morphology close to the time-point of the evaluation of the markers was the most effective. Prediction accuracy was highest in case of the morphological information in the single time-point data on the final day (prediction performance: OCT3/4 = 86.4%, rBC2LCN = 93.0%) (Fig. 5D).

This detailed analysis of morphological information indicated that the undifferentiated markers used to evaluate iPSC colonies were most strongly correlated with colony morphology at their final stage, and early morphological prediction does not reliably show high accuracy.

DISCUSSION

In the practical cell manufacturing process, the importance of cell quality maintenance is a crucial issue. Because cells are alive and undergo changes and the culture process is long and complex, examining the quality of the products only at the final stage is insufficient. As a breakthrough for overcoming this difficulty, non-invasive and real-time monitoring technology using images shows great potential and advantages for evaluating cell manufacturing processes.

We focused on examining two aspects of image analysis for iPSC manufacturing. The first involved applying image analysis for quantitatively evaluating the techniques/skills used in iPSC culture, which is a practical issue that has been neglected in previous studies. We investigated the cellular morphological changes that occurred in cells upon their dissociation by pipetting. Particularly, in clump-type seeding, controlling cellular aggregation size is critical for iPSC quality (24). The second was to improve the image analysis of iPSC colonies by time-course colony tracking and determine the effectiveness of using tracked morphological information for quality evaluation. In cell manufacturing processes, the yield of cells is very important. If the cell culture process generates an unexpectedly low yield, the final cultured cells can be discarded before packaging when the total cell number is a critical final criterion of manufacturing. Even when this is not the case, if the yield is low, unexpected additional culture processes may be required, greatly altering the total culture costs. By analyzing the cell yield, colony tracking analysis revealed two types of advantageous data that can be neglected in the image data without tracking. The first dataset was that of the individual colony growth rates. Irregularly expanding/shrinking colonies were easily identified. Moreover, such colonies rarely appeared because of the pipetting effect. The second dataset was that of the timing of colony growth. When all colonies were tracked individually, the start of their growth could be identified. Using growth-starting point information, when the individual colonies reached a certain size (diameter of 225 μm in our setting), we stratified the total growth curves and evaluated the impact of pipetting stress. In our tracking analysis, the pipetting impact, which is not clearly understood, had a larger impact on the start of the growth of fast-recognized cells, rather than lowering the individual cell growth rates. Moreover, fast-recognized colonies were the major population among the obtained colonies, suggesting that the production efficiency of iPSC colonies within the homogeneous size range can be controlled by optimizing the cell dissociation process. If homogeneous fast-recognized cells can be seeded with less stress, productivity and homogeneity may increase. Our data shows that when optimizing techniques or cell strains, tracking analysis is an informative and quantitative tool for evaluating cell quality.

Colony tracking analysis, which can reflect the total time-course history of each colony, was also effective for setting a criterion for standard behavior of colonies. Such continuously obtained data of colonies were used to hypothetically define the standard growth sizes. When the sizes can be defined statistically, the difference between cell strains or their sensitivity to stress can be quantified. However, the statistically defined standard range of colony size does not guarantee biological marker expression, but is an important scale for understanding the stability of manufacturing performance.

Our staining results indicate that even if the cell yield is high with a certain number of colonies, cell quality can differ greatly if the colonies vary in size. Therefore, controlling the final iPSC colony size within a certain range is important for reducing the risk of immature or overgrown colonies, which can reduce product quality. Although iPSC colony size is an important feature, it is difficult to control the standard range of final colony size. The most difficult aspect is that even if the colony size distribution at the end of the culture can be measured by simple image analysis, such end-point data cannot indicate why and when such colonies deviated from the normal range. End-point image analysis does not explain why

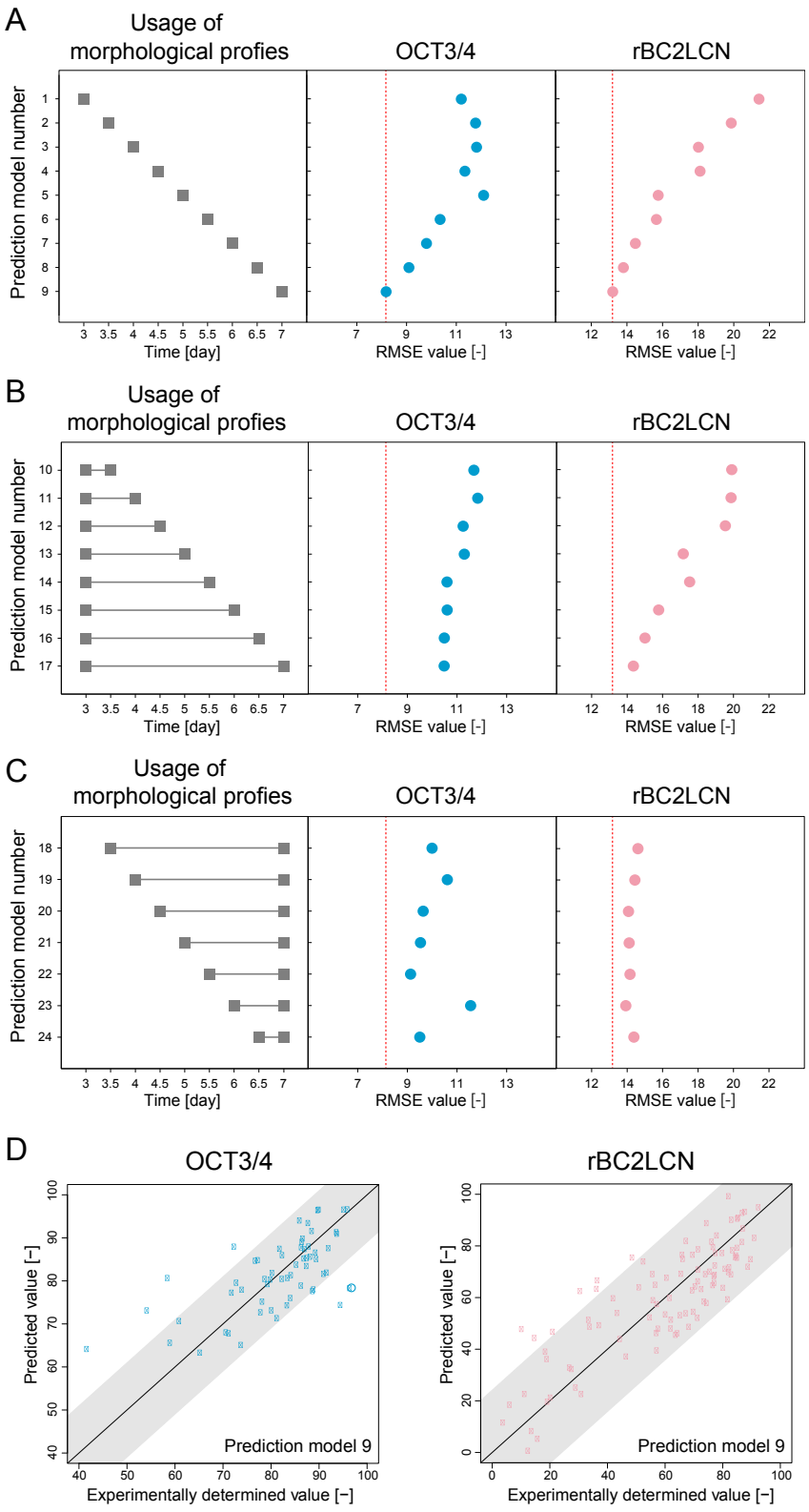

FIG. 5. Investigation of morphological information content for predicting two types of undifferentiation marker expression potentials on day 7 (OCT3/4 and rBC2LCN). (A) Comparison of prediction performances using individual time-point morphological profiles. (B) Comparison of prediction performance using different length of window-size of accumulated morphological profiles from the earlier period. (C) Comparison of prediction performance using different lengths of window-size of accumulated morphological profiles from the later period. The plots indicate the root mean square error (RMSE) value. Each model is numbered on the side of the figures. The illustration of the box and line (shaded) indicates the usage of morphological profiles for input information to predict the future marker staining rate. Blue plots indicate the RMSE values of OCT3/4 staining area predictions, and pink plots indicate RMSE values of rBC2LCN staining area predictions. The red dotted vertical line on the plots indicate the minimum RMSE value (model 9). (D) Predictive performance of OCT3/4 or rBC2LCN staining area (day 7) by morphological profiles from day 7 (model 9). X-axis: experimentally determined values, Y-axis: predicted values from the morphological profiles. The shaded region on the plot indicates the possible deviation area affected by experimental error (defined as the mean ± SD of the experimental data). If the plots are in this region, the prediction is highly reliable.

TABLE 1. Weighted morphological parameters in the best performance prediction model (prediction model 9 shown in Fig. 5).

Time (day)	Category	Parameter	Coefficient value ($\times 10^{-2}$)	
			OCT3/4	rBC2LCN
7	Peripheral information	Area	2.81	−5.44
7		Compactness	−5.21	0
7		Equivalent radius	0	0
7		Inner radius	−85.7	−6.89
7		Perimeter	0	4.78
7		Rod like width	−3.43	8.44
7		Shape factor	−1.89	1.52
7	Intensity	CV	0	0
7		Mean	0.743	12.4
7		Median	0	−9.76
7		Standard deviation	−3.16	2.23
7	Texture	Correlation	15.5	19.7
7		Energy	0	−22.4
7		Entropy	−18.4	0
7		Homogony	−62.0	−8.45
7		Inertia	−28.5	−0.00210

small colonies increase in the population, whether their growth rate decreased, or if the start of their growth was delayed. For such investigations, colony tracking analysis is a powerful tool for interpreting the kinetics of colony growth.

When tracks were evaluated as representative colonies at the end of the culture period, the distribution information obtained was important for manufacturing. One parameter is the distribution bias, which reveals information regarding colony growth characteristics. The other parameter is the population complexity, which reflects homogeneity. From this information (Fig. S3), the level of pipetting stress was found to have different effects on different cell lines, indicating that pipetting should be optimized to each cell line to minimize the rate of deviated clones.

Using the colony tracking data, which consists of information linking the morphology and marker staining data of the same colonies, highly accurate marker staining rate prediction models were constructed. OCT3/4 is a marker expressed in the nucleus and rBC2LCN is a surface polysaccharide marker (25). Although these markers are expressed in different cellular locations, we found that the use of multiple morphological parameters can result in prediction models with similarly high accuracy. When comparing multiple morphological information, the prediction models using a single parameter (area at day 7) did not show high prediction performance (Fig. S4). From the highly weighted parameters in the prediction model, we found that not only size-related parameters, but also intensity- and texture-related parameters were important (Table 1).

Unexpectedly, in our detailed analysis of the time-course information content, the prediction performance of marker staining results (day 7) was found to be maximized when using the most recent morphological examination (day 7). Compared to morphological analysis of mesenchymal stem cells (26), neural stem cells (27), or myoblasts (28), the accumulated time-course morphological information did not contribute to prediction performance. Therefore, although the quality of other two-dimensionally cultured cells can be predicted at early time-points, that of iPSC colonies could not. Based on the size-dependency in the marker staining results shown in Fig. S2, the predicted markers (OCT3/4 and rBC2LCN) were confirmed to require colony maturation. Therefore, for these markers, colony morphology only started to correlate with their expression only during their last period of culture. These data suggest that iPSCs require continuous monitoring until the final period of cell yield, and our colony tracking technology can be applied to monitor the total culture process.

Although colony tracking analysis in this study provided deeper information from the same image data, there are several disadvantages to this method. First, tracking data can include false-positive records. In general, objects in different time-course images are linked as a track based on their locations in the image. When images are not well-focused, the first object recognition step can fail, and an incorrect object can be included in the track. Additionally, when cells become confluent or are densely seeded, linking of neighboring/fused colonies in the track may occur. To avoid such mis-tracking, careful confirmation of each image is important. Second, because of the technical limitations of image processing, tracking of time-course colonies cannot cover all colonies. If the numbers of fields of view is insufficient, only a few tracks will be available to obtain data over a long time-course. At the end of the time-course, most colonies begin to fuse as they grow, and thus many tracks are diminished or show an irregular record because of mis-tracking. To efficiently use track information as statistical representatives, optimization of the seeding density and observation window, combined with automated large-scale image acquisition, is essential.

In summary, our results indicate that colony tracking analysis of individual iPSC colonies provides detailed information for visualizing and analyzing changes in the cellular status during the cell culture process. Combined with the results of morphological parameter usage for iPSC quality prediction, image-based analysis was found to be a powerful supportive tool in iPSC manufacturing. Additionally, our results suggested that colony tracking can be applied to design or optimize cell culture protocols in cell manufacturing facilities. To further expand our method, we will next apply our image-based analysis for culturing standard iPSC lines for clinical trials and patient-derived iPSCs.

Supplementary data to this article can be found online at https://doi.org/10.1016/j.jbiosc.2019.01.011.

ACKNOWLEDGMENTS

This research was supported by the Development of Cell Production and Processing Systems for Commercialization of Regenerative Medicine program of the Japan Agency for Medical Research and Development (AMED), grants-in-aid from the New Energy and Industrial Technology Development Organization (NEDO) (09C46036a), and the Japan Science and Technology Agency (JST) Program for Creating STart-ups from Advanced Research and Technology (START Program) program. We also greatly thank for the collaboration and research support from Nikon Corporation, and the instrumental support and advices for the imaging and image processing by Yasujiro Kiyota, Takayuki Uozumi, and Hiroaki Kii from the Stem Cell Business Development, Technology Solution Sector, the Healthcare Business Unit, Nikon Corporation.

References

1. **Skalova, S., Svadlakova, T., Qureshi, W. M. S., Dev, K., and Mokry, J.:** Induced pluripotent stem cells and their use in cardiac and neural regenerative medicine, Int. J. Mol. Sci., **16**, 4043–4067 (2015).
2. **Kondo, Y., Toyoda, T., Inagaki, N., and Osafune, K.:** IPSC technology-based regenerative therapy for diabetes, J. Diabetes Investig., **9**, 234–243 (2018).
3. **Cao, L., Tan, L., Jiang, T., Zhu, X.-C., and Yu, J.-T.:** Induced pluripotent stem cells for disease modeling and drug discovery in neurodegenerative diseases, Mol. Neurobiol., **52**, 244–255 (2015).
4. **Bruyneel, A. A., McKeithan, W. L., Feyen, D. A., and Mercola, M.:** Will ipsc-cardiomyocytes revolutionize the discovery of drugs for heart disease? Curr. Opin. Pharmacol., **42**, 55–61 (2018).
5. **Elitt, M. S., Barbar, L., and Tesar, P. J.:** Drug screening for human genetic diseases using ipsc models, Hum. Mol. Genet., **27**, 89–98 (2018).
6. **Jenkins, M. J. and Farid, S. S.:** Human pluripotent stem cell-derived products: advances towards robust, scalable and cost-effective manufacturing strategies, Biotechnol. J., **10**, 83–95 (2015).

7. **Amit, M., Chebath, J., Margulets, V., Laevsky, I., Miropolsky, Y., Shariki, K., Peri, M., Blais, I., Slutsky, G., Revel, M., and Itskovitz-Eldor, J.:** Suspension culture of undifferentiated human embryonic and induced pluripotent stem cells, Stem Cell Rev. Rep., **6**, 248–259 (2010).
8. **Dos Santos, F. F., Andrade, P. Z., Da Silva, C. L., and Cabral, J. M. S.:** Bioreactor design for clinical-grade expansion of stem cells, Biotechnol. J., **8**, 644–654 (2013).
9. **Serra, M., Brito, C., Correia, C., and Alves, P. M.:** Process engineering of human pluripotent stem cells for clinical application, Trends Biotechnol., **30**, 350–359 (2012).
10. **Matsuoka, F., Takeuchi, I., Agata, H., Kagami, H., Shiono, H., Kiyota, Y., Honda, H., and Kato, R.:** Morphology-based prediction of osteogenic differentiation potential of human mesenchymal stem cells, PLoS One, **8**, e55082 (2013).
11. **Sasaki, H., Takeuchi, I., Okada, M., Sawada, R., Kanie, K., Kiyota, Y., Honda, H., and Kato, R.:** Label-free morphology-based prediction of multiple differentiation potentials of human mesenchymal stem cells for early evaluation of intact cells, PLoS One, **9**, e93952 (2014).
12. **Kawai, S., Sasaki, H., Okada, N., Kanie, K., Yokoshima, S., Fukuyama, T., Honda, H., and Kato, R.:** Morphological evaluation of nonlabeled cells to detect stimulation of nerve growth factor expression by lyconadin B, J. Biomol. Screen, **21**, 795–803 (2016).
13. **Maherali, N. and Hochedlinger, K.:** Guidelines and techniques for the generation of induced pluripotent stem cells, Cell Stem Cell, **3**, 595–605 (2008).
14. **Courtot, A.-M., Magniez, A., Oudrhiri, N., Féraud, O., Bacci, J., Gobbo, E., Proust, S., Turhan, A. G., and Bennaceur-Griscelli, A.:** Morphological analysis of human induced pluripotent stem cells during induced differentiation and reverse programming, Biores. Open Access, **3**, 206–216 (2014).
15. **Tokunaga, K., Saitoh, N., Goldberg, I. G., Sakamoto, C., Yasuda, Y., Yoshida, Y., Yamanaka, S., and Nakao, M.:** Computational image analysis of colony and nuclear morphology to evaluate human induced pluripotent stem cells, Sci. Rep., **4**, 6996 (2014).
16. **Suga, M., Kii, H., Niikura, K., Kiyota, Y., and Furue, M. K.:** Development of a monitoring method for nonlabeled human pluripotent stem cell growth by time-lapse image analysis, Stem Cells Transl. Med., **4**, 720–730 (2015).
17. **Tsankov, A. M., Akopian, V., Pop, R., Chetty, S., Gifford, C. A., Daheron, L., Tsankova, N. M., and Meissner, A.:** A qpcr scorecard quantifies the differentiation potential of human pluripotent stem cells, Nat. Biotechnol., **33**, 1182–1192 (2015).
18. **Müller, F. J., Schuldt, B. M., Williams, R., Mason, D., Altun, G., Papapetrou, E. P., Danner, S., Goldmann, J. E., Herbst, A., Schmidt, N. O., and other 3 authors:** A bioinformatic assay for pluripotency in human cells, Nat. Methods, **8**, 315–317 (2011).
19. **Avior, Y., Biancotti, J. C., and Benvenisty, N.:** TeratoScore: assessing the differentiation potential of human pluripotent stem cells by quantitative expression analysis of teratomas, Stem Cell Rep., **4**, 967–974 (2015).
20. **Kato, R., Matsumoto, M., Sasaki, H., Joto, R., Okada, M., Ikeda, Y., Kanie, K., Suga, M., Kinehara, M., Yanagihara, K., and other 8 authors:** Parametric analysis of colony morphology of non-labelled live human pluripotent stem cells for cell quality control, Sci. Rep., **6**, 34009 (2016).
21. **Nagasaka, R., Matsumoto, M., Okada, M., Sasaki, H., Kanie, K., Kii, H., Uozumi, T., Kiyota, Y., Honda, H., and Kato, R.:** Visualization of morphological categories of colonies for monitoring of effect on induced pluripotent stem cell culture status, Regen. Ther., **6**, 41–51 (2017).
22. **Nagasaka, R., Gotou, Y., Yoshida, K., Kanie, K., Shimizu, K., Honda, H., and Kato, R.:** Image-based cell quality evaluation to detect irregularities under same culture process of human induced pluripotent stem cells, J. Biosci. Bioeng., **123**, 642–650 (2017).
23. **Xie, Y., Wang, F., Puscheck, E. E., and Rappolee, D. A.:** Pipetting causes shear stress and elevation of phosphorylated stress-activated protein kinase/jun kinase in preimplantation embryos, Mol. Reprod. Dev., **74**, 1287–1294 (2007).
24. **Bauwens, C. L., Peerani, R., Niebruegge, S., Woodhouse, K. A., Kumacheva, E., Husain, M., and Zandstra, P. W.:** Control of human embryonic stem cell colony and aggregate size heterogeneity influences differentiation trajectories, Stem Cell, **26**, 2300–2310 (2008).
25. **Tateno, H., Toyota, M., Saito, S., Onuma, Y., Ito, Y., Hiemori, K., Fukumura, M., Matsushima, A., Nakanishi, M., Ohnuma, K., and other 5 authors:** Glycome diagnosis of human induced pluripotent stem cells using lectin microarray, J. Biol. Chem., **286**, 20345–20353 (2011).
26. **Imai, Y., Yoshida, K., Matsumoto, M., Okada, M., Kanie, K., Shimizu, K., Honda, H., and Kato, R.:** In-process evaluation of culture errors using morphology-based image analysis, Regen. Ther., **9**, 15–23 (2018).
27. **Fujitani, M., Huddin, N. S., Kawai, S., Kanie, K., Kiyota, Y., Shimizu, K., Honda, H., and Kato, R.:** Morphology-based non-invasive quantitative prediction of the differentiation status of neural stem cells, J. Biosci. Bioeng., **124**, 351–358 (2017).
28. **Ishikawa, K., Yoshida, K., Kanie, K., Omori, K., and Kato, R.:** Morphology-based analysis of myoblasts for prediction of myotube formation, SLAS Discov., **24**, 47–56 (2019).